The 8th Laser Ceramics Symposium, 2012
International Symposium on Transparent Ceramics for Photonic Applications
Ceramics characterization - 4

PM 14:30-15:00
Dec. 5, 2012

Fundamental sciences in orientation control process for anisotropic laser ceramics

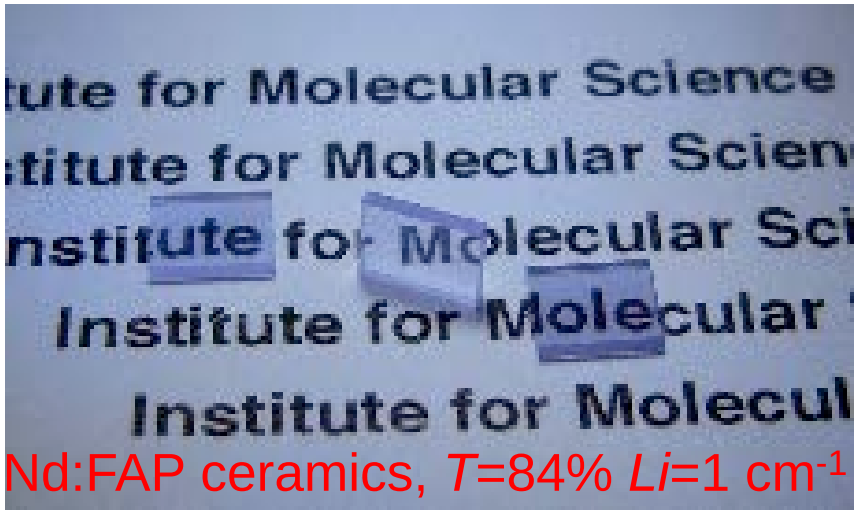

Nd:FAP ceramics, T=84% Li=1 cm^{-1}

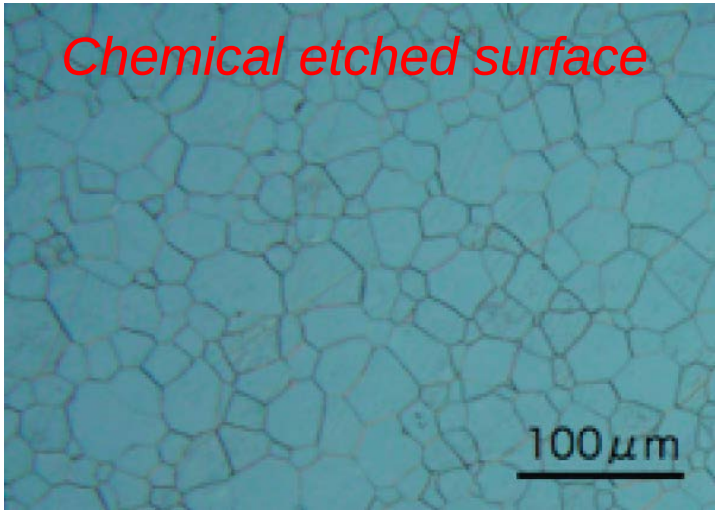

Yoichi Sato, Jun Akiyama, and Takunori Taira

Institute for Molecular Science
38 Nishigonaka, Myodaiji, Okazaki 444-8585 Japan
yoichi@ims.ac.jp, taira@ims.ac.jp

Our activity on cubic laser ceramics

Please visit for detailed information: http://taira-web.ims.ac.jp/

- Concept of composite ceramics (1998)
- Superiority to single crystalline media (2000)
- In-band pumping & Emission quenching (2001)
- Thermally induced depolarization (2002)
- Disordered garnet ceramics (2003)
- First fs-pulse mode-locking (2004)
- Highest power density in CW operation (2005)
- Precise thermal conductivity (2007)
- Laser ignitors for automobile engines (2011)

…. etc.

Agenda

Study on anisotropic laser ceramics

- Objective
- Origin of magnetic anisotropy
- Basic design rules for alignment control
  - (a) Slip-casting under magnetic field
  - (b) Preferential grain growth during sintering
- Experimental confirmation
- Conclusion

Evolutions of laser gain media

	Single crystal	Ceramics
Cubic	RE:YAG High optical quality Most reliable Small size	RE:YAG ceramics Large aperture Composite material High tensile strength
Non-cubic	RE:YVO_4 RE:Apatite High efficiency Large cross section Small size	**RE:anisotropic ceramics**

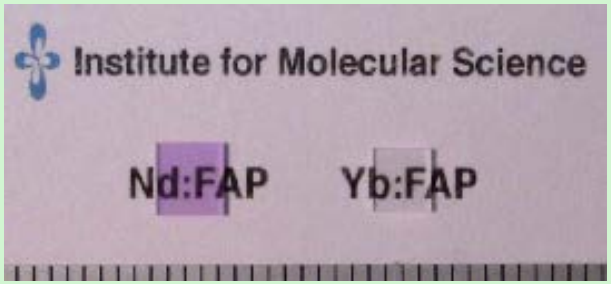

Desire for large FAP media

RE:anisotropic ceramics have been strongly expected !

Yb:S-FAP (hexagonal) single crystals*

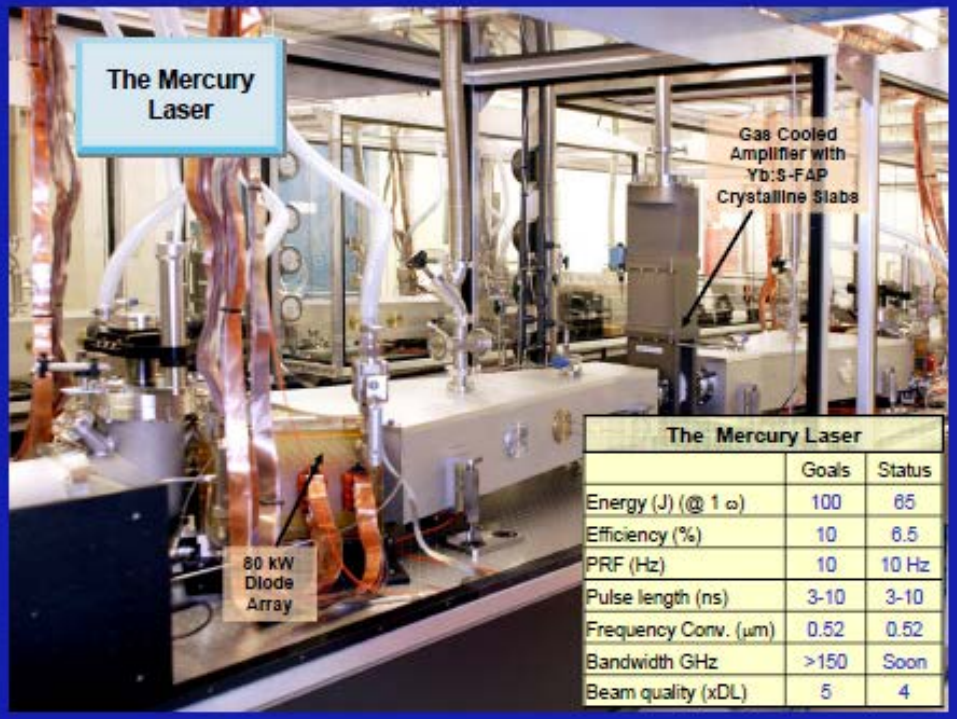

The Mercury Laser	Goals	Status
Energy (J) (@ 1 ω)	100	65
Efficiency (%)	10	6.5
PRF (Hz)	10	10 Hz
Pulse length (ns)	3-10	3-10
Frequency Conv. (μm)	0.52	0.52
Bandwidth GHz	>150	Soon
Beam quality (xDL)	5	4

Grow 7 cm diameter crystal

Excellent optical properties:
- High absorption efficiency
- High emission cross-section
- Long lifetime

* K. I. Schaffers et al., IWCGT-4, May 18-25, 2008

Laser fusion driver (LLNL: Mercury Laser)

Anisotropic laser ceramics

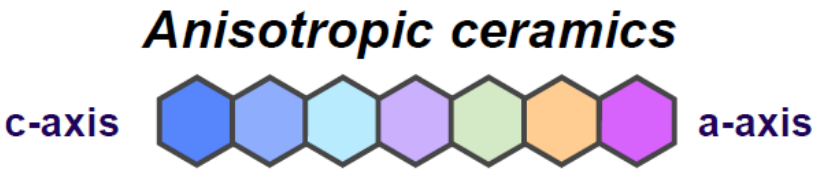

Polycrystal with birefringence

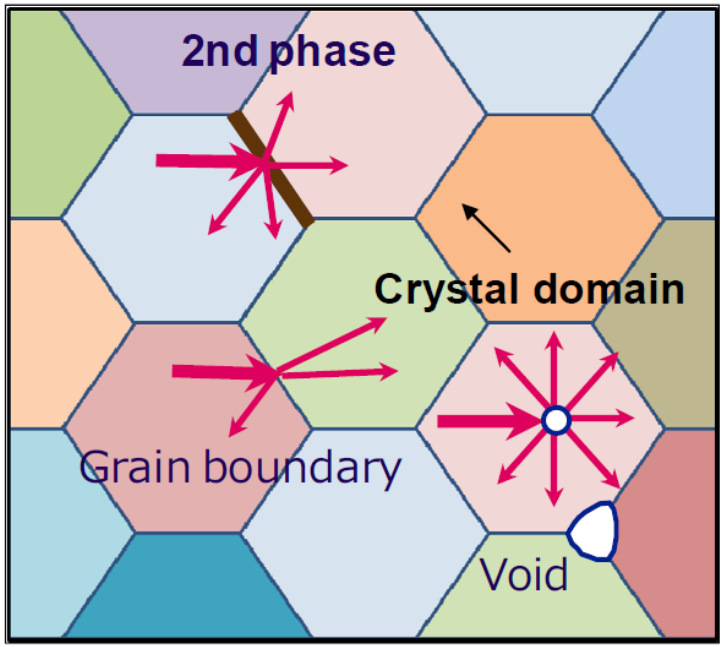

Scattering source

Orientation controlled polycrystal

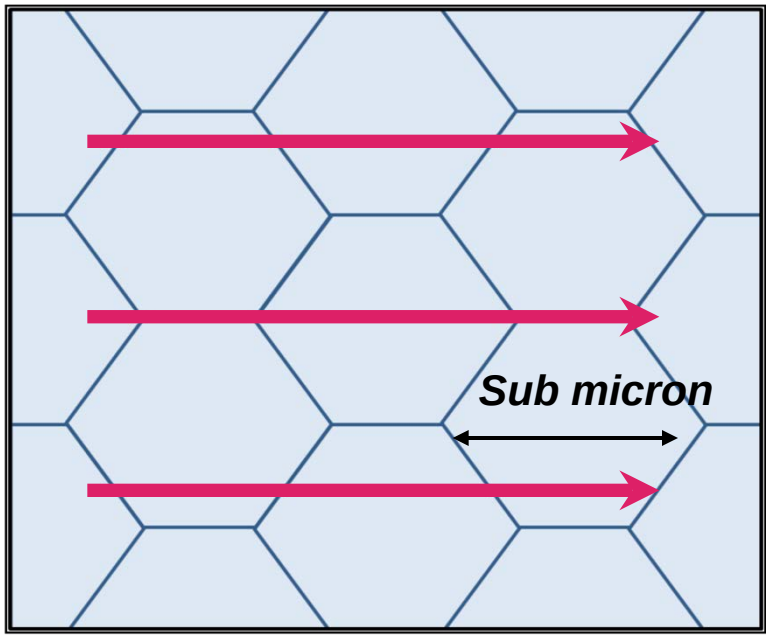

Uni-axially Orientated material

Micro-domain control

- Principles -

Applied external field controls the domain characteristics

Gibbs energy

$$dG = -SdT + \sum_i \mu_i dN_i - \sum_i V_i \gamma_{GB} d\left(\frac{1}{r_i}\right) + V \sum_{i,j} e_{ij} d\sigma_{ij} - \boldsymbol{P} \cdot d\boldsymbol{E} - \boldsymbol{M} \cdot d\boldsymbol{B}$$

Crystal growth (traditional)

Grain growth

Stress control

Electric control

Magnetic control

I. Shoji et al., Appl. Phys. Lett.**77**, 939 (2000).

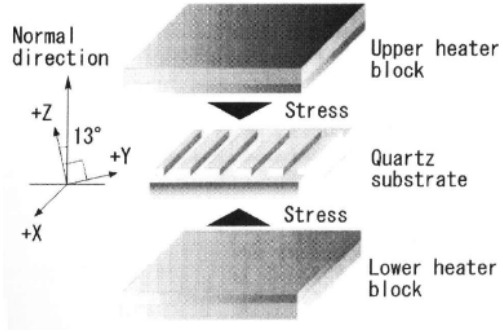

M. Harada et al., J. Materi. Res. **19**, 969 (2004).

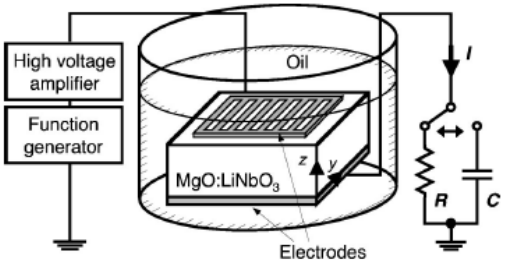

H. Ishizuki et al., Appl. Phys. Lett.**82**, 4062 (2003).

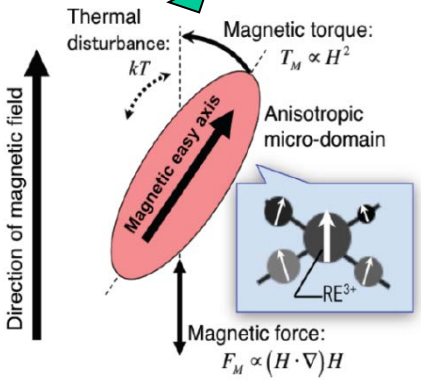

J. Akiyama et al., Opt. Lett. **35**, 3598 (2010).

Recent progress in magnetic control

Electromagnetic processing (1998~)

- Technology of orientation control for NON-magnetic materials.
- Superconducting magnet is required for material processing (**B>10T**).

Antiferromagnetic materials
Paramagnetic materials
Diamagnetic materials

Structural control by spin-orbit interaction (2009~)

- Micro domain structure control for GIANT-MICRO PHOTONICS.
- Enhancing magnetic anisotropy in non-magnetic materials.
- Electromagnet can produce enough magnetic field (**B~1T**).

Ref. J. Akiyama, Y. Sato, and T.Taira: Opt. Lett. 35, 3598 (2010)

Recent progress in orientation control

Ele

s.

ials

Str

)

ICS.

3598 OPTICS LETTERS / Vol. 35, No. 21 / November 1, 2010

Laser ceramics with rare-earth-doped anisotropic materials

Jun Akiyama,* Yoichi Sato, and Takunori Taira

Laser Research Center for Molecular Science, Institute for Molecular Science, 38 Nishigonaka, Myodaiji, Okazaki 444-8585, Japan

**Corresponding author: akiyama@ims.ac.jp*

Received August 17, 2010; accepted September 13, 2010;
posted October 5, 2010 (Doc. ID 133465); published October 21, 2010

The fabrication of laser-grade anisotropic ceramics by a conventional sintering process is not possible owing to optical scattering at randomly oriented grain boundaries. In this Letter, we report the first (to our knowledge) realization of transparent anisotropic ceramics by using a new crystal orientation process based on large magnetic anisotropy induced by 4*f* electrons. By slip casting in a 1.4 T magnetic field and subsequent heat treatments, we could successfully fabricate laser-grade calcium fluorapatite ceramics with a loss coefficient of 1.5 cm^{-1}. © 2010 Optical Society of America

OCIS codes: 140.3380, 140.3390, 160.3380, 160.5690.

Advancements in the design and development of polycrystalline ceramic laser media during the past decade [1–6] have contributed to the enhancement of the power density and functionality of solid-state lasers. These devices have various scientific, medical, and industrial

field of 10 T [12–15]. Figure 1 presents the new method proposed for orientation control of the microdomain structure in RE^{3+}-doped anisotropic laser ceramics. The spin–orbit interaction of the 4*f* electrons of an RE^{3+} ion strongly enhances the net magnetic anisotropy $\Delta\chi$,

Ref. J. Akiyama, Y. Sato, and T.Taira: Opt. Lett. 35, 3598 (2010)

The 1st Anisotropic Ceramic Laser

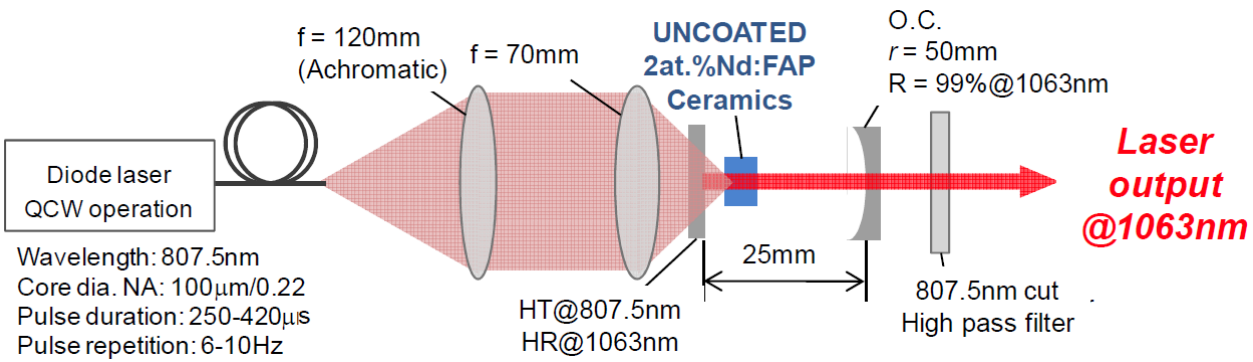

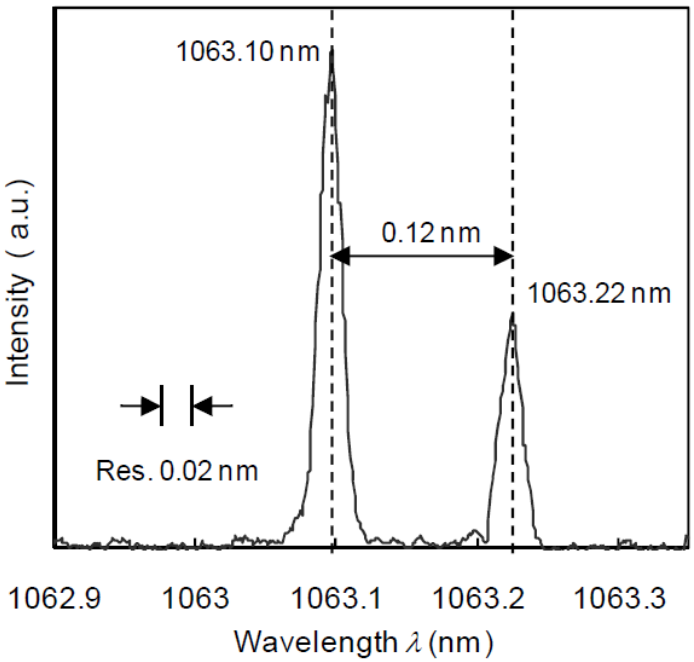

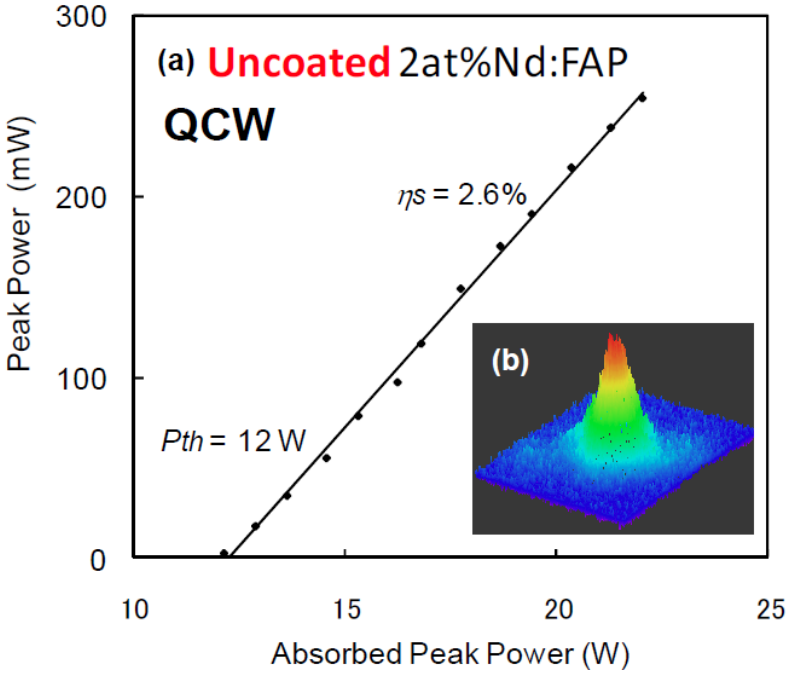

Ref. J. Akiyama, Y. Sato, and T.Taira: Appl. Phys. Express 4, 022703 (2011)

The 1st Anisotropic Ceramic Laser

Applied Physics Express 4 (2011) 022703
DOI: 10.1143/APEX.4.022703

Laser Demonstration of Diode-Pumped Nd^{3+}-Doped Fluorapatite Anisotropic Ceramics

Jun Akiyama*, Yoichi Sato, and Takunori Taira

Laser Research Center for Molecular Science, Institute for Molecular Science, Okazaki, Aichi 444-8585, Japan

Received December 4, 2010; accepted December 25, 2010; published online January 24, 2011

We report the first demonstration of a diode-pumped anisotropic ceramic laser that uses microdomain-controlled neodymium-doped hexagonal fluorapatite [Nd^{3+}:$Ca_{10}(PO_4)_6F_2$, Nd:FAP] polycrystalline ceramics as the gain medium, which were fabricated by the rare-earth-assisted magnetic grain-orientation control method, as a step toward achieving giant micro photonics. The laser delivers 1063.10 and 1063.22 nm output beams when pumped with a central wavelength of 807.5 nm and a 2 nm bandwidth diode laser operating in quasi-continuous-wave (QCW) mode. We obtained a maximum QCW peak power of 255 mW with an uncoated 2 at. % Nd:FAP material. © 2011 The Japan Society of Applied Physics

Trivalent rare-earth-doped $Y_3Al_5O_{12}$ (YAG, cubic) crystals are one of the most popular and most promising solid-state laser materials because of their high quantum efficiency and superior mechanical properties. Moreover, the design and development of YAG ceramic media over the past decade has greatly contributed to the improvement in the power density and functionality of solid-state laser devices,[1–8] and the industrial and scientific applications of these devices have extended to inertia

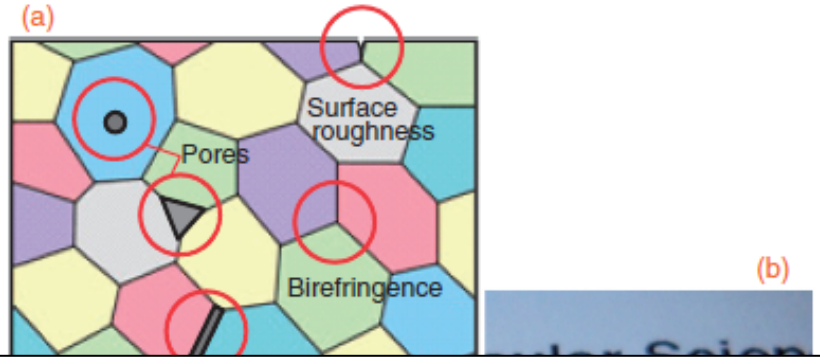

Wavelength λ (nm)

Absorbed Peak Power (W)

Ref. J. Akiyama, Y. Sato, and T.Taira: Appl. Phys. Express 4, 022703 (2011)

Objective

Since possibility was already proved, the standardization and the further improvement are next targets.

In order to improve anisotropic laser ceramics,
It is necessary to show clearly what has caused un-uniformity in micro domain (=grain) structure.

<u>This work is aiming to find the perspective of …</u>

Uniformity of crystal alignment in grain axis.

(1) The origin of magnetic anisotropy

If $\Delta\chi$ become designable, we can perform orientation control more perfect.

Micro-domain control

- Principles -

Applied external field controls the domain characteristics

Gibbs energy

$$dG = -SdT + \sum_i \mu_i dN_i - \sum_i V_i \gamma_{GB} d\left(\frac{1}{r_i}\right) + V \sum_{i,j} e_{ij} d\sigma_{ij} - \boldsymbol{P} \cdot d\boldsymbol{E} - \boldsymbol{M} \cdot d\boldsymbol{B}$$

Crystal growth (traditional)

Grain growth

Stress control

Electric control

Magnetic control

I. Shoji et al., Appl. Phys. Lett.**77**, 939 (2000).

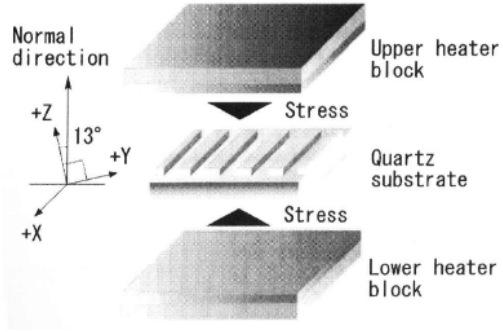

M. Harada et al., J. Materi. Res. **19**, 969 (2004).

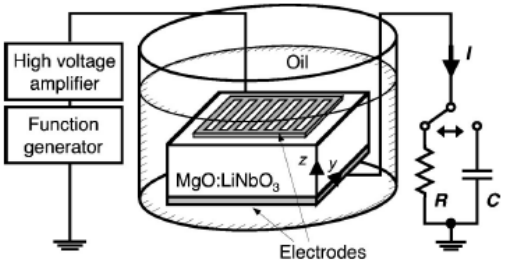

H. Ishizuki et al., Appl. Phys. Lett.**82**, 4062 (2003).

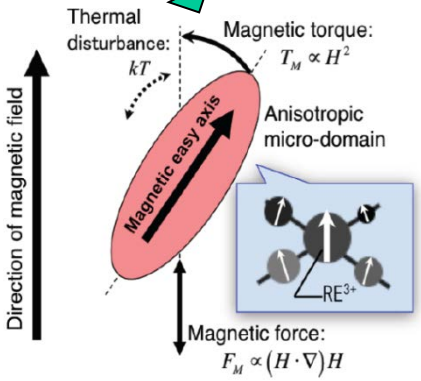

J. Akiyama et al., Opt. Lett. **35**, 3598 (2010).

Micro-domain control

- Principles of rare-earth assisted magnetic orientation control -

Applied external field controls the domain characteristics

Gibbs energy

$$dG = -SdT + \sum_i \mu_i dN_i - \sum_i V_i \gamma_{GB} d\left(\frac{1}{r_i}\right) + V \sum_{i,j} e_{ij} d\sigma_{ij} - \boldsymbol{P} \cdot d\boldsymbol{E} - \boldsymbol{M} \cdot d\boldsymbol{B}$$

Crystal growth (traditional)

Grain growth

Stress control

Electric control

Magnetic control

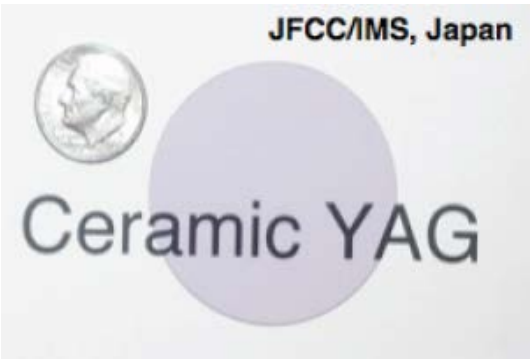

I. Shoji et al., Appl. Phys. Lett.**77**, 939 (2000).

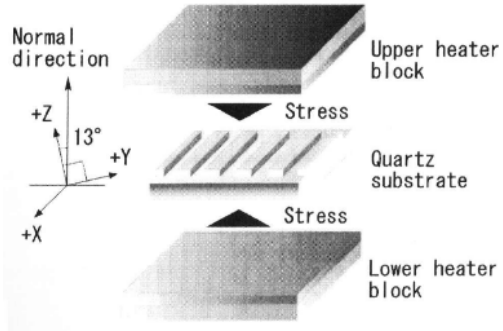

M. Harada et al., J. Materi. Res. **19**, 969 (2004).

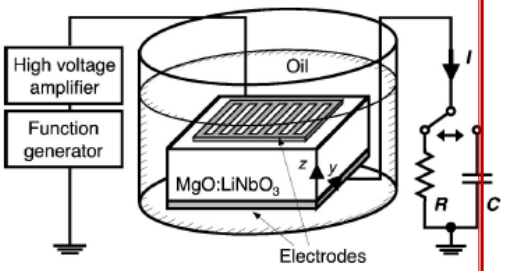

H. Ishizuki et al., Appl. Phys. Lett.**82**, 4062 (2003).

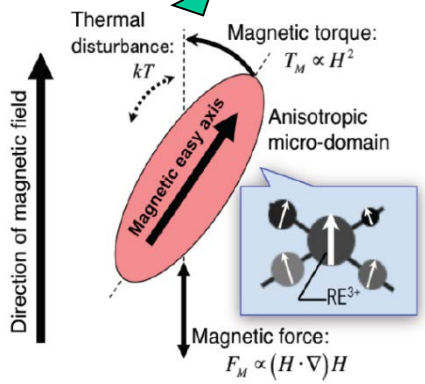

J. Akiyama et al., Opt. Lett. **35**, 3598 (2010).

Magneto-crystalline anisotropy

$$dG = -\boldsymbol{M} \cdot d\boldsymbol{B}$$

Magnetization

$$\boldsymbol{M} = \frac{V}{\mu_0}\begin{pmatrix} \chi_{11} & \chi_{12} & \chi_{13} \\ \chi_{21} & \chi_{22} & \chi_{23} \\ \chi_{31} & \chi_{32} & \chi_{33} \end{pmatrix}\boldsymbol{B}$$

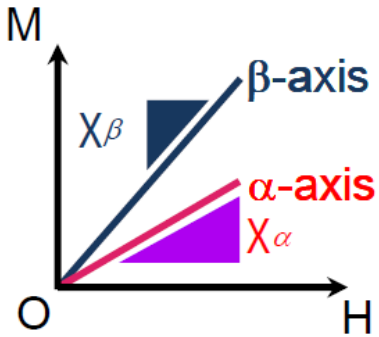

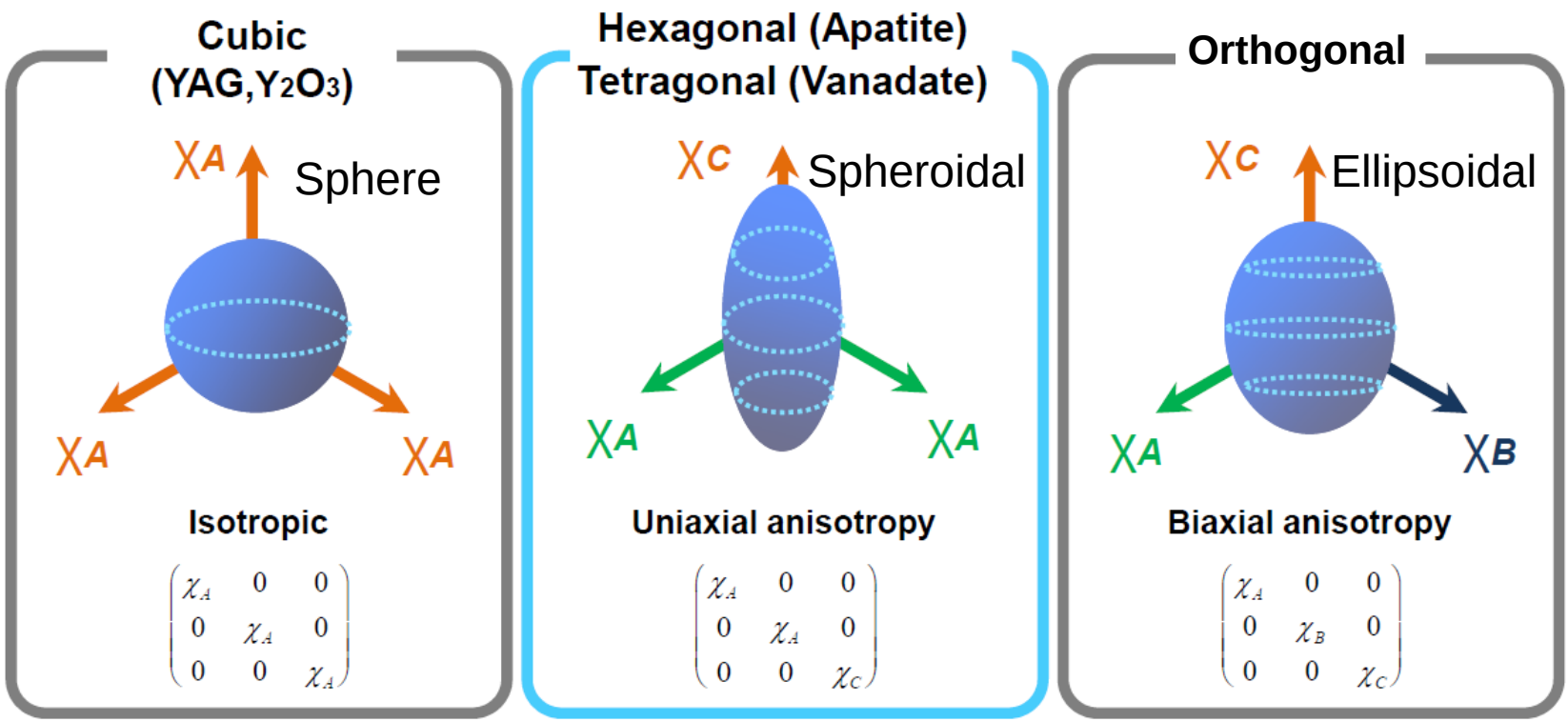

Magnetism in various materials

			Examples	Susceptibility	Processing
Magnetic materials	Strong magnetism	Ferro magnetism	Fe, Co, Ni, Gd	**10^1 ~10^4**	Weak ***B*** Applicable
		Ferri magnetism	Fe_3O_4		
Non-magnetic materials	Feeble magnetism	Antiferro magnetism	FeO, $FeCl_2$	**10^{-3} ~10^{-7}**	Strong ***B*** required
		Para magnetism	Rare earth		
	Diamagnetism		**Laser host materials**	**$< 10^{-7}$**	Extremely strong ***B*** required

Magnetism in various materials

			Examples	Susceptibility	Processing
Magnetic materials	Strong magnetism	Ferro magnetism	Fe, Co, Ni, Gd	10^{1} ~10^{4}	Weak ***B*** Applicable
		Ferri magnetism	Fe_3O_4		
Non-magnetic materials	Feeble magnetism	Antiferro magnetism	FeO, $FeCl_2$	10^{-3} ~10^{-7}	Strong ***B*** required **DOPING**
		Para magnetism	Rare earth		
	Diamagnetism		**Laser host materials**	10^{-4} ~10^{-7}	Strong ***B*** required

Magnetic anisotropy in RE:crystals

- Magnetic moment of 4f electrons -

Dirac equation

$$\left[i\hbar \frac{\partial}{\partial t} + e\phi - c\boldsymbol{\alpha} \cdot (\boldsymbol{p} + e\boldsymbol{A}) - \beta mc^2 \right] \psi = 0$$

Pauli approximation

$$\left[\frac{(\boldsymbol{p} + e\boldsymbol{A})^2}{2m} + \frac{e}{m} \boldsymbol{s} \cdot \boldsymbol{B} - e\phi \right] \begin{pmatrix} \phi_1 \\ \phi_2 \end{pmatrix} = E' \begin{pmatrix} \phi_1 \\ \phi_2 \end{pmatrix}$$

$$\left[\frac{\boldsymbol{p}^2}{2m} + \frac{e^2}{8m} \left\{ r^2 B^2 - (\boldsymbol{r} \cdot \boldsymbol{B})^2 \right\} + \frac{m_B}{\hbar} (\boldsymbol{l} + 2\boldsymbol{s}) \cdot \boldsymbol{B} - e\phi \right] \begin{pmatrix} \phi_1 \\ \phi_2 \end{pmatrix} = E' \begin{pmatrix} \phi_1 \\ \phi_2 \end{pmatrix}$$

Lamor diamagnetism

Magnetic potential

$$dG = -\boldsymbol{M} \cdot d\boldsymbol{B}$$

Magnetic moment for electron: $\boldsymbol{m} = -\frac{m_B}{\hbar} (\boldsymbol{l} + 2\boldsymbol{s}) - \frac{e^2}{4m} \left[r^2 \boldsymbol{B} - (\boldsymbol{r} \cdot \boldsymbol{B}) \boldsymbol{r} \right]$

Magnetic moment under low magnetic field for rare earth ion:

Bohr magneton

Total angular momentum

$$\boldsymbol{m}_e = -g_J \frac{m_B}{\hbar} \boldsymbol{J}$$

Lande's g-factor

Plank's constant

Magnetic anisotropy in RE:crystals

- Magnetic susceptibility of 4f electrons -

Zeeman energy

$$G = -\boldsymbol{M} \cdot \boldsymbol{B}$$

Mother function of free energy

$$G = -kT \ln \sum_i \exp\left[-\frac{E_i}{kT}\right]$$

Second order perturbation

$$E_i(\boldsymbol{B}) = E_i(0) - g_J m_B \langle i | \boldsymbol{J} | i \rangle \boldsymbol{B} + (g_J m_B)^2 \boldsymbol{B}^2 \sum_j \frac{\left|\langle j | \boldsymbol{J} | i \rangle\right|^2}{E_j(0) - E_i(0)}$$

Energy level of state i perturbed by Zeeman energy

Definition of susceptibility

$$\chi = \mu_0 \left.\frac{\partial \boldsymbol{M}}{\partial \boldsymbol{B}}\right|_{B=0} = \mu_0 \left.\frac{\partial^2 G}{\partial \boldsymbol{B}^2}\right|_{B=0} = \frac{\mu_0}{k_B T}\left\langle \left(\frac{\partial E_i}{\partial \boldsymbol{B}}\right)^2 \right\rangle - \frac{\mu_0}{k_B T}\left\langle \frac{\partial E_i}{\partial \boldsymbol{B}} \right\rangle^2 + \mu_0 \left\langle \frac{\partial^2 E_i}{\partial \boldsymbol{B}^2} \right\rangle$$

Magnetic susceptibility

$$\chi = \mu_0 \frac{(g_J m_B)^2}{kT} \sum_{i<j \in {}^{2S+1}L} \left[\left|\langle i | J_Z | i \rangle\right|^2 f_i - 2k_B T \frac{f_j - f_i}{E_j - E_i} \left|\langle j | J_Z | i \rangle\right|^2 \right]$$

Fractional population of level-*i*

Magnetic anisotropy in RE:crystals

- Origin of magnetic anisotropy of 4f electrons in crystals -

Magnetic anisotropy:

$$\Delta\chi = \chi_{//} - \chi_{\perp} = \mu_0 \frac{(g_J m_B)^2}{kT} \sum_{i<j} \left[\left(\left|\langle i | J_z^{//} | i \rangle\right|^2 - \left|\langle i | J_z^{\perp} | i \rangle\right|^2 \right) f_i - 2k_B T \left(\left|\langle j | J_z^{//} | i \rangle\right|^2 - \left|\langle j | J_z^{\perp} | i \rangle\right|^2 \right) \frac{f_j - f_i}{E_j - E_i} \right]$$

Magnetic anisotropy is defined by the matrix elements of total angular momentum along the direction of applied magnetic field.

The origin of magnetic anisotropy is the dependency of J_z in the crystal field.

Narrow bandwidth of 4f electrons brings non-zero value of J_z

(2) Basic design rules for alignment control

Clarifying the limit of alignment control by slip-casting under magnetic field.

(a) Alignment control by slip-casting under magnetic field

Clarifying the limit in the alignment control of primary particles by slip-casting under magnetic field.

Kinetics of orientation control by *B*

- Equation of motion for particles under magnetic field -

Torque *T* is derived by differentiating potential with respect to θ.

$$\boldsymbol{T} = -\boldsymbol{e}_\varphi \frac{\partial G}{\partial \theta} + \boldsymbol{e}_\theta \frac{1}{\sin\theta}\frac{\partial G}{\partial \varphi} = -\frac{V\Delta\chi}{2\mu_0} B^2 \sin 2\theta \boldsymbol{e}_\varphi$$

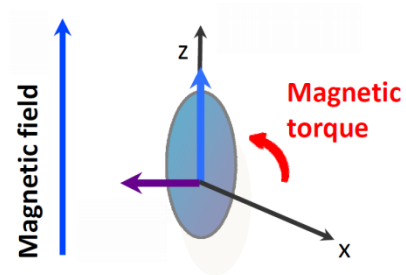

Inertial moment

Coefficient of viscosity

$$I\frac{d^2\theta}{dt^2} + 6\eta V\frac{d\theta}{dt} = -\frac{V\Delta\chi}{2\mu_0} B^2 \sin 2\theta$$

Assumption : inertial force is negligible

$$\tan\theta = \tan\theta_0 \exp\left(-\frac{t}{\tau}\right) \qquad \tau = \frac{6\mu_0\eta}{\Delta\chi B^2}$$

Langevin equation

Random force by Brownian motion

$$I\frac{d^2\theta}{dt^2} + 6\eta V\frac{d\theta}{dt} = -\frac{V\Delta\chi}{2\mu_0} B^2 \sin 2\theta + R(t)$$

R limits the temporal form and the strength of ***B***.

- High viscosity brings the benefit of large *V*, however it also causes longer process time.
- Low viscosity brings the benefit of shorter process time, however it limits the floating time of core particles.

Orientation distribution in slurry

- Theoretical treatment -

Under thermal equilibrium → Boltzmann distribution

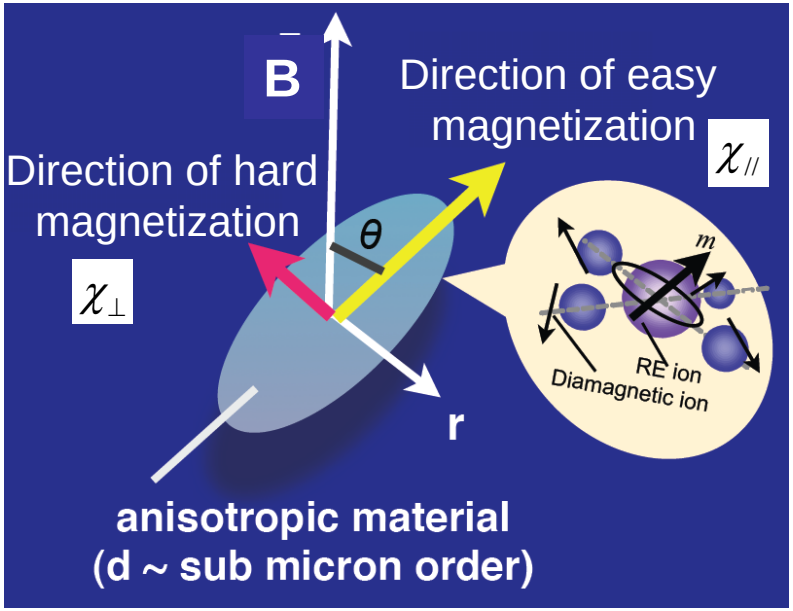

Distribution function f_{eq} for the orientation of primary particles in slurry under equilibrium

$$f_{eq}(\theta,\varphi)d\Omega = N\frac{\exp\left(-\frac{G}{kT}\right)d\Omega}{\int \exp\left(-\frac{G}{kT}\right)d\Omega'}$$

$$\approx \frac{N}{4\pi}\frac{2B^2+B_{\min}{}^2}{B_{\min}{}^2}(\cos\theta)^{\frac{2B^2}{B_{\min}{}^2}}d\Omega$$

Magnetostatic energy G

Volume of particles

Magnetic field

$$G = -\int_0^B \boldsymbol{M}\cdot d\boldsymbol{B} = -\frac{VB^2}{2\mu_0}\left(\chi_{//}\cos^2\theta + \chi_{\perp}\sin^2\theta\right)$$

$$= -\frac{VB^2}{2\mu_0}\left(\chi_{//} - \Delta\chi\sin^2\theta\right)$$

permeability

$$G_{\perp}(B_{\min}) - G_{//}(B_{\min}) = kT \;\Rightarrow\; B_{\min} = \sqrt{\frac{2\mu_0 kT}{V\Delta\chi}}$$

Anisotropy in magnetic susceptibility (= $\chi_{//}$ - χ_{+})

Orientation distribution in slurry

- Calculation for process design -

Under thermal equilibrium with magnetic field

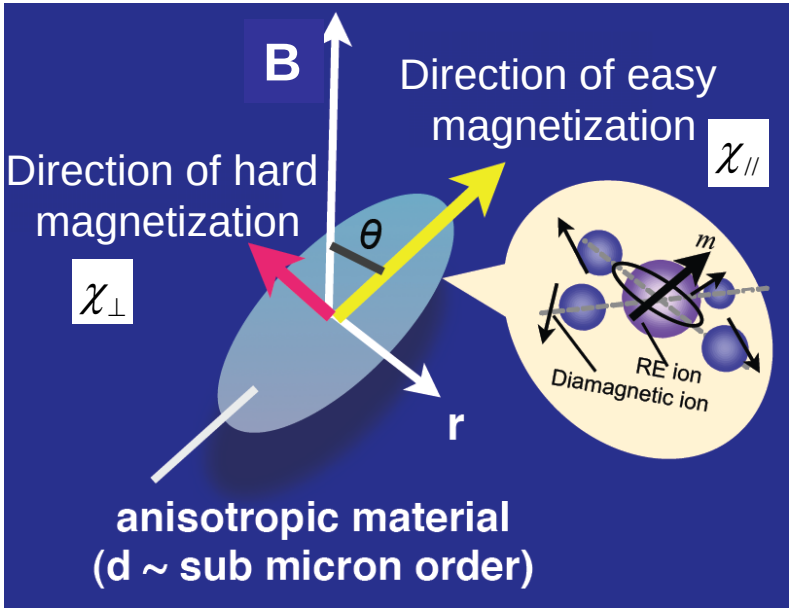

Distribution probability *P* of primary particles in slurry under equilibrium shows not perfect alignment.

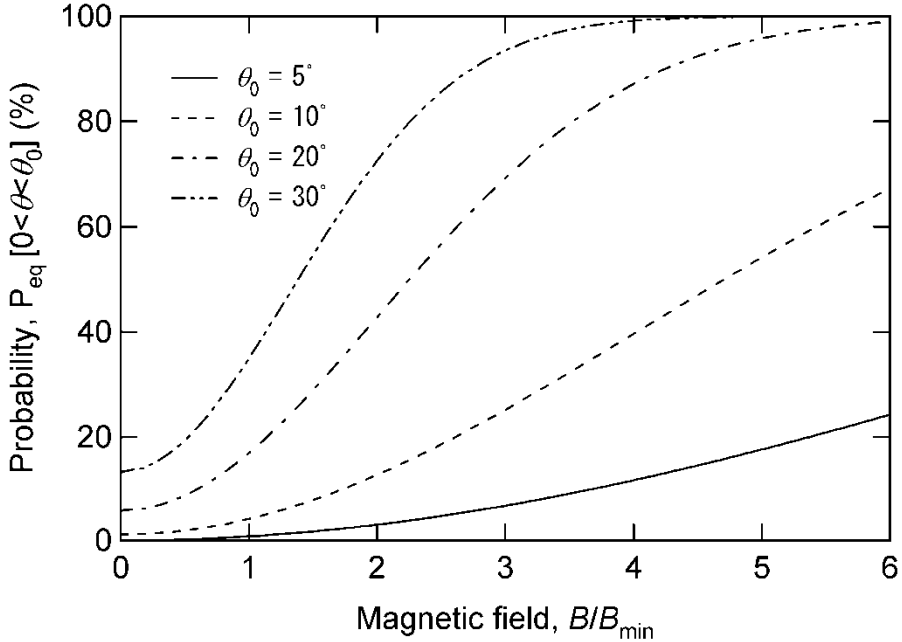

$$P[0 \le \theta \le \theta_0]$$

$$= \frac{2\pi}{N}\int_0^{\theta_0} f_{eq}(\theta,\varphi)\sin\theta d\theta + \frac{2\pi}{N}\int_{\pi-\theta_0}^{\pi} f_{eq}(\theta,\varphi)\sin\theta d\theta$$

$$\approx \left[1-(\cos\theta)^{\frac{2B^2+B_{min}{}^2}{B_{min}{}^2}}\right]$$

$$B_{min} = \sqrt{\frac{2\mu_0 kT}{V\Delta\chi}}$$

Larger *V*
Larger $\Delta\chi$
requires.

(b) Preferential grain growth during sintering

How we can improve the alignment of green body composed of primary particles with roughly distributed directions.

Micro-domain control

- Principles -

Applied external field controls the domain characteristics

Gibbs energy

$$dG = -SdT + \sum_i \mu_i dN_i - \sum_i V_i \gamma_{GB} d\left(\frac{1}{r_i}\right) + V \sum_{i,j} e_{ij} d\sigma_{ij} - \boldsymbol{P} \cdot d\boldsymbol{E} - \boldsymbol{M} \cdot d\boldsymbol{B}$$

Crystal growth (traditional)

Grain growth

Stress control

Electric control

Magnetic control

I. Shoji et al., Appl. Phys. Lett.**77**, 939 (2000).

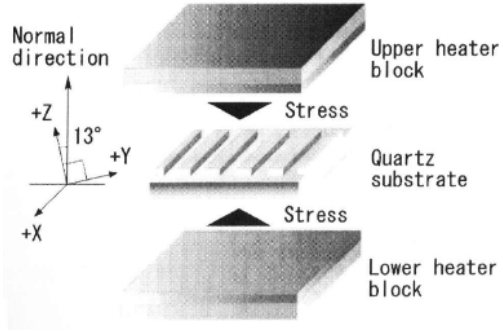

M. Harada et al., J. Materi. Res. **19**, 969 (2004).

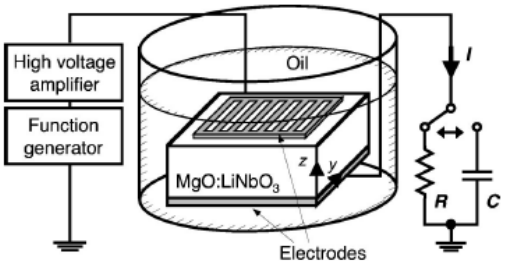

H. Ishizuki et al., Appl. Phys. Lett.**82**, 4062 (2003).

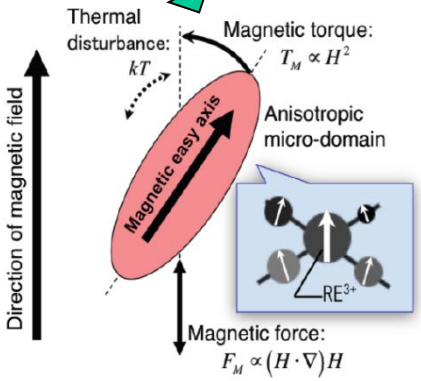

J. Akiyama et al., Opt. Lett. **35**, 3598 (2010).

Micro-domain control

- Principles of preferential grain growth -

Applied external field controls the domain characteristics

Gibbs energy

$$dG = -SdT + \sum_i \mu_i dN_i - \sum_i V_i \gamma_{GB} d\left(\frac{1}{r_i}\right) + V \sum_{i,j} e_{ij} d\sigma_{ij} - \boldsymbol{P} \cdot d\boldsymbol{E} - \boldsymbol{M} \cdot d\boldsymbol{B}$$

Crystal growth (traditional)

Grain growth

Stress control

Electric control

Magnetic control

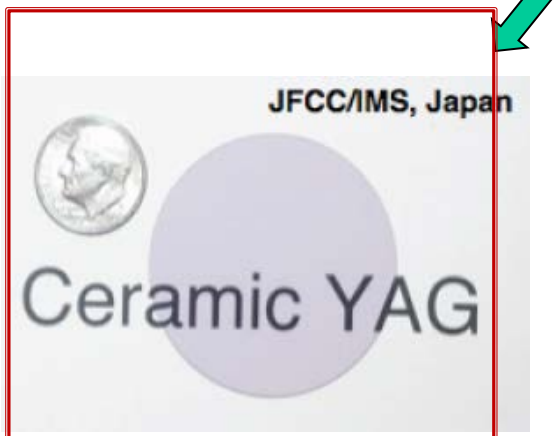

I. Shoji et al., Appl. Phys. Lett.**77**, 939 (2000).

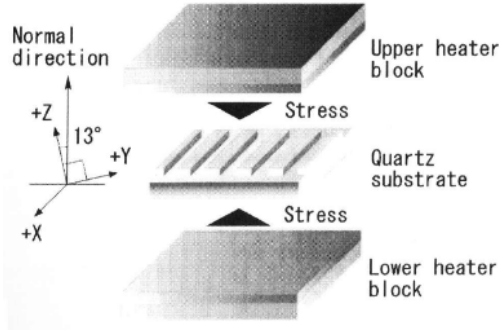

M. Harada et al., J. Materi. Res. **19**, 969 (2004).

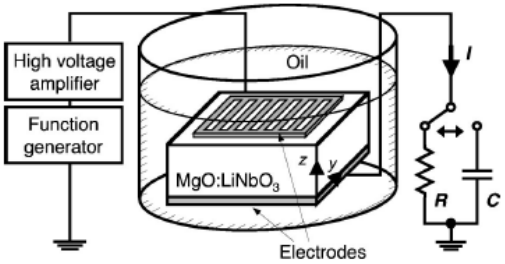

H. Ishizuki et al., Appl. Phys. Lett.**82**, 4062 (2003).

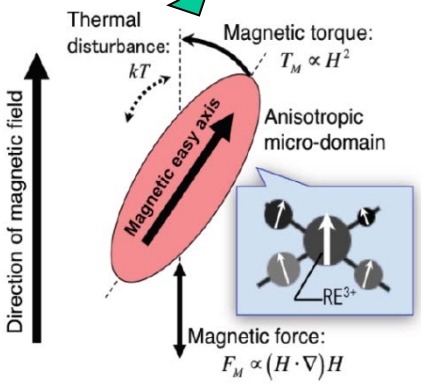

J. Akiyama et al., Opt. Lett. **35**, 3598 (2010).

Kinetics of preferential grain growth

Gibbs free energy

$$dG = -\sum_k \gamma_g V_k d\left(\frac{1}{r_k}\right) \approx \frac{4\pi}{3}\gamma_g \sum_k r_k dr_k \quad ,$$

(at initial condition under sintering)

Bounding condition:

$$\sum_k r_k{}^2 dr_k = 0 \ .$$

(Only 2 grains condition)

$$dG = \frac{4\pi}{3}\gamma_g\left(1 - \frac{r_1}{r_2}\right) r_1 dr_1 \ .$$

The grain with larger size become larger,
and the grain with smaller size becomes smaller

Preferential grain growth

- Principle for re-alignment under sintering -

Uniform particles in sintering

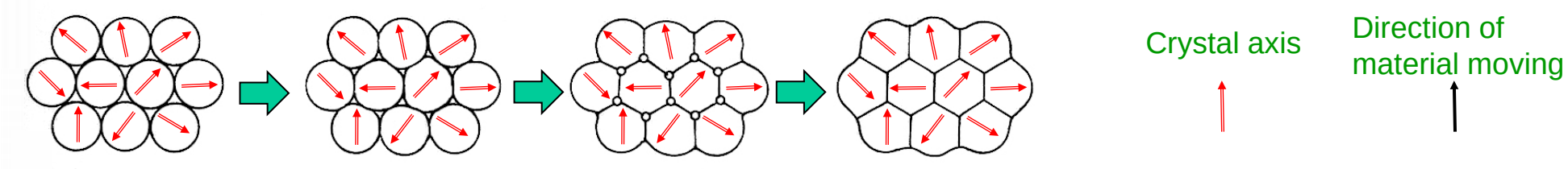

Particles with various sizes in sintering

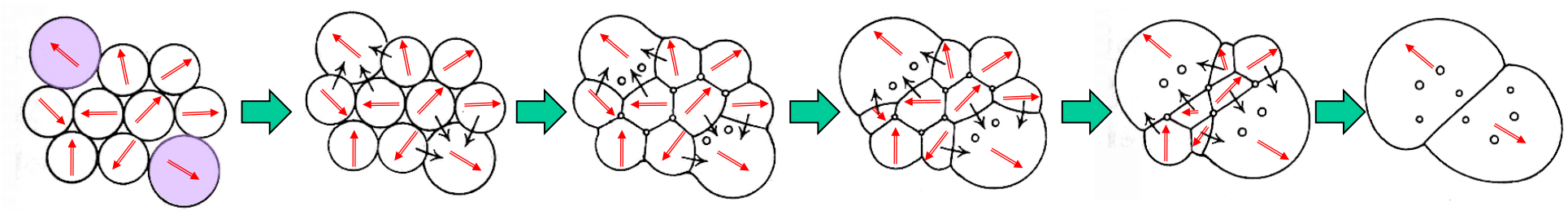

Particles with various sizes in sintering with suppressed grain growth

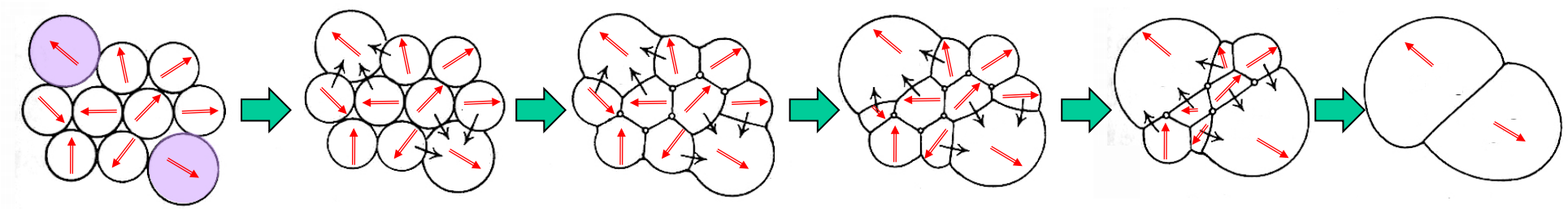

If there are larger particles than others, **they rule the total direction**.

Preferential grain growth

- Core particles in preferential growth -

Core particles of preferential grain growth are (grain size)^3 / (particle size) ^{3} ~ **below 1%** of particles.

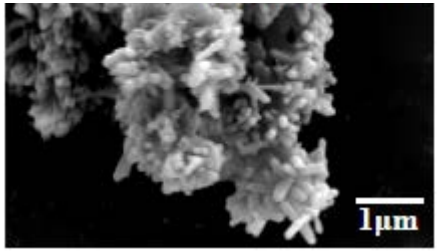

Primary particles in aggregates (~1μm)

Sintering

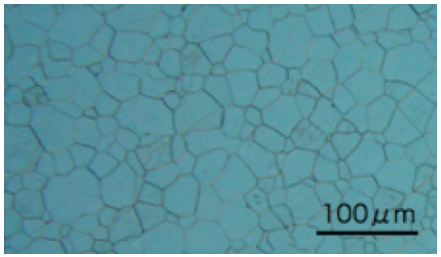

Grains in polycristals (>10μm)

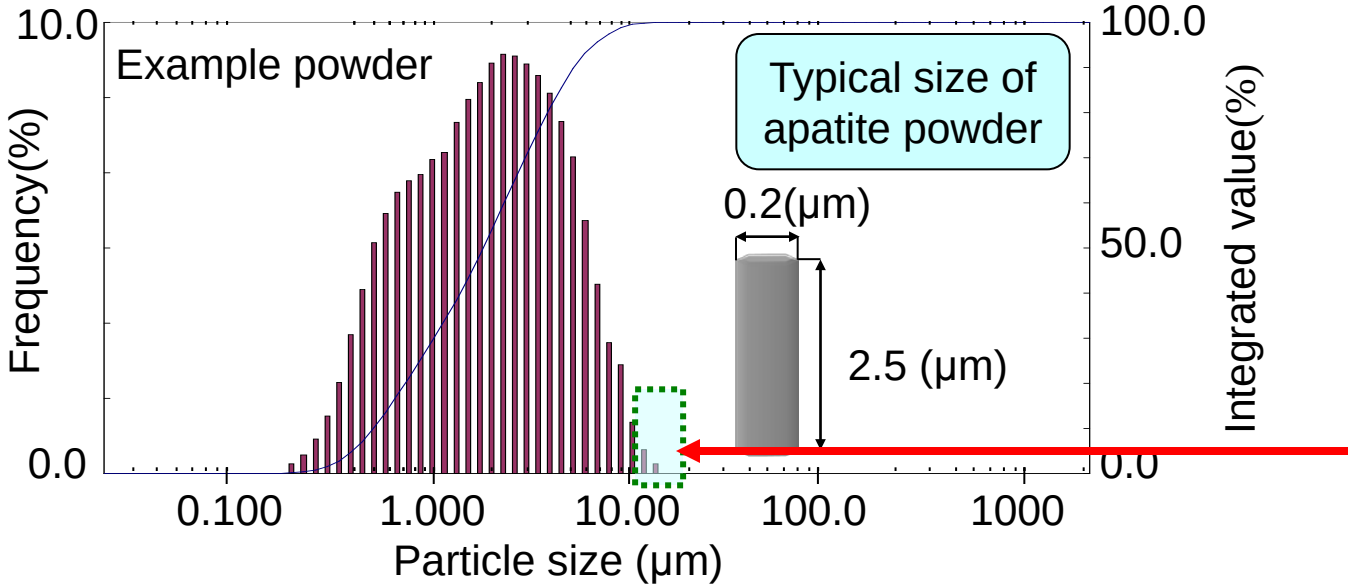

Core particles of preferential growth has over 10 times larger diameter than mean particles.

Preferential grain growth

- Improvement of grain alignment during sintering -

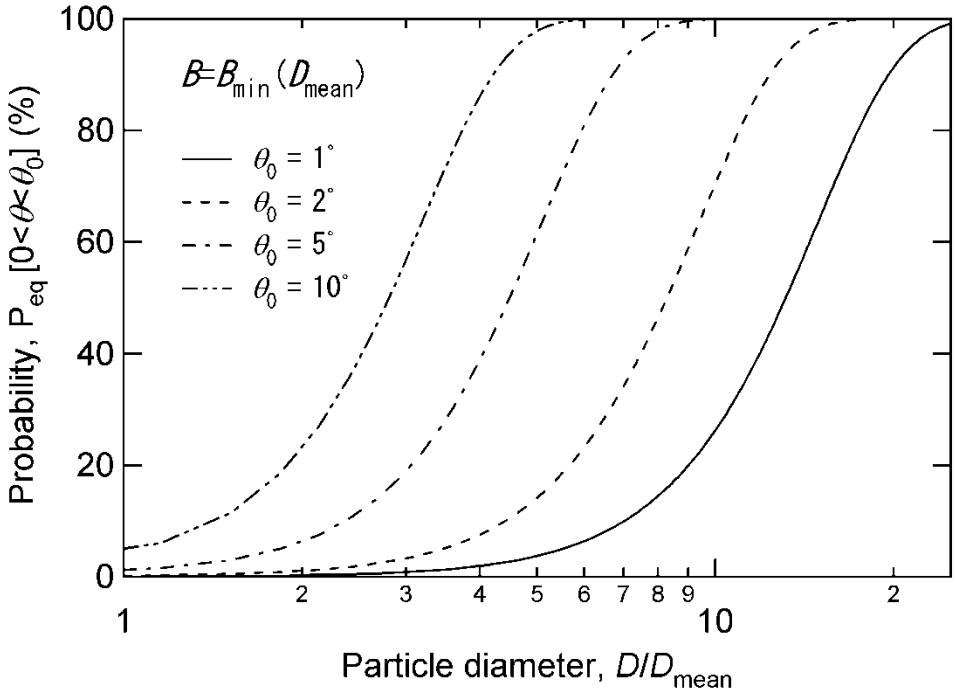

Assumed condition:

$$B = B_{\min}\left(D_{\text{mean}}\right) \qquad B = \sqrt{\frac{2\mu_0 kT}{V_{\text{mean}}\Delta\chi}}$$

Particles with

D_{mean} : $P\left[0 \le \theta \le 5°\right] \approx 1\%$

$7.4D_{\text{mean}}$: $P\left[0 \le \theta \le 5°\right] \approx 95\%$

$23D_{\text{mean}}$: $P\left[0 \le \theta \le 1°\right] \approx 95\%$

Even if *B* is comparable to B_{min} for mean particles, core particles for grain growth can be well aligned by slip-casting.

It is important for making good aligned ceramics to design the nature of raw powders.

Confirmation of orientation control

Experimental orientation control process

Magnetic anisotropy in YVO_4

Evaluation of magnetic anisotropy

@280K, r=230 nm	1.8at.% Yb:YVO_4	Undoped YVO_4
$\Delta\chi$ [emu/mol] @ 7T	3.9×10^{-5}	7.1×10^{-6}
$\Delta\chi$ [SI unit] @ 7T	8.0×10^{-7}	1.5×10^{-7}
B_{min} [T]	1.4	3.3

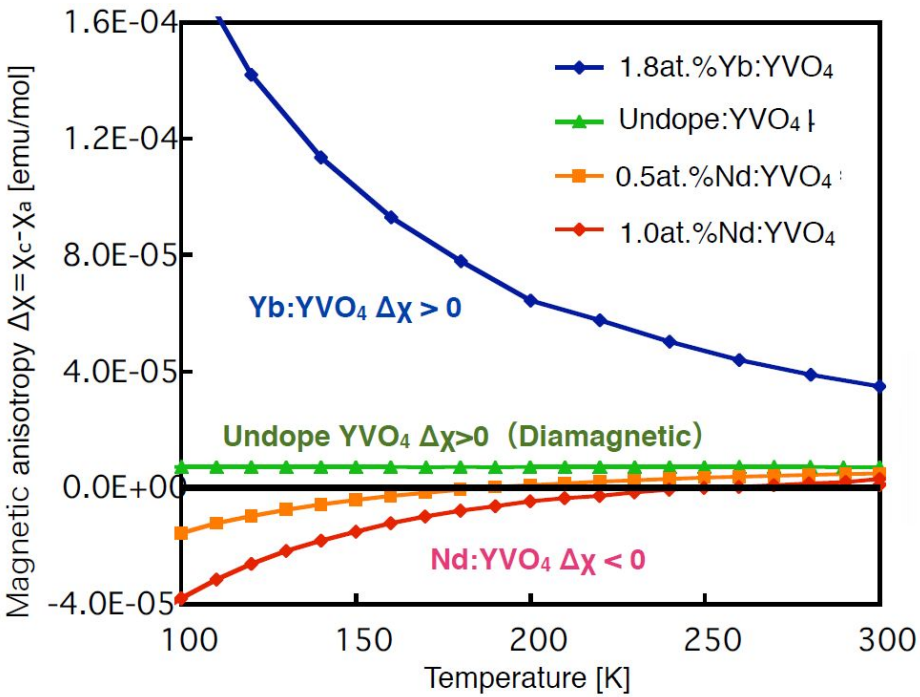

No need of superconductive magnet.

Electromagnet can supply enough strong magnetic field

(**MPMS-7, Quantum Design**)

Orientation control of ceramic grains

Process for orientation control

↓

Slip-casting under magnetic field

↓

Preferential grain growth by sintering

↓

Anisotropic laser ceramics

1st step : Slip-casting under magnetic field

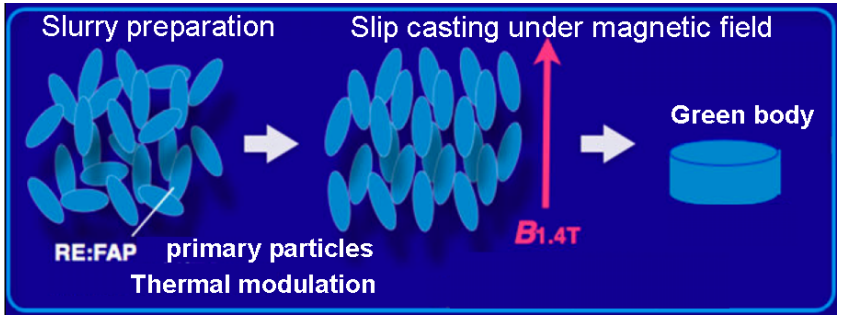

Rough alignments due to thermal modulation

2nd step : Preferential grain growth

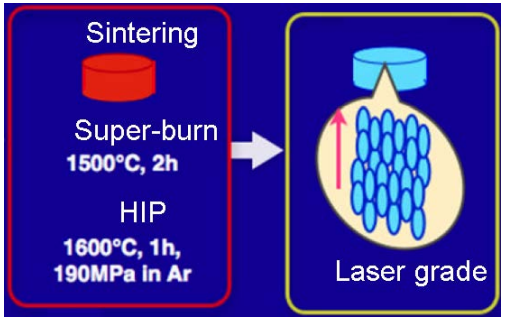

Nearly perfect alignment can be realized.

It requires the control of orientation distribution of green during slip-casting.

Flow-chart for manufacturing

RE:FAP particles
(RE: Nd^{3+}, Yb^{3+})

Distilled Water

Deflocculant (polymer)

Mixing and Milling <6h

Slip casting
under magnetic field (1.4T) <6h

Drying 24h

1st sintering
1600℃, 2h, in Air

2nd sintering
Hot Isostatic Pressing
1500℃, 1h, 190MPa, in Ar

Polishing

Traditional EMP requires
>10T magnetic field
by super-conducting magnet

Electric magnet (B_{MAX}=1.5T)

Crystal orientation of RE:FAP ceramics

Highly oriented Nd:FAP materials have been successfully obtained by 1.4T magnetic field imposition.

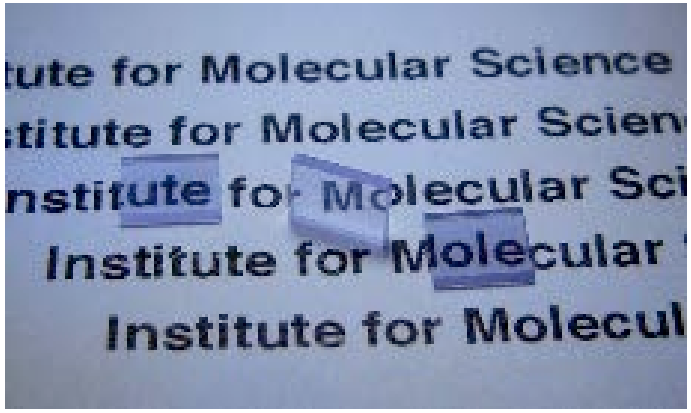

Nd:FAP ceramics, T=84% Li=1 cm^{-1}

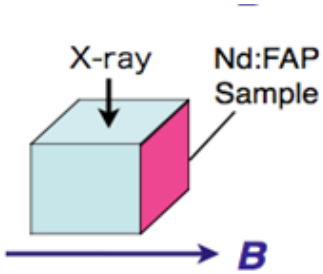

(RINT-Ultima III, Rigaku)

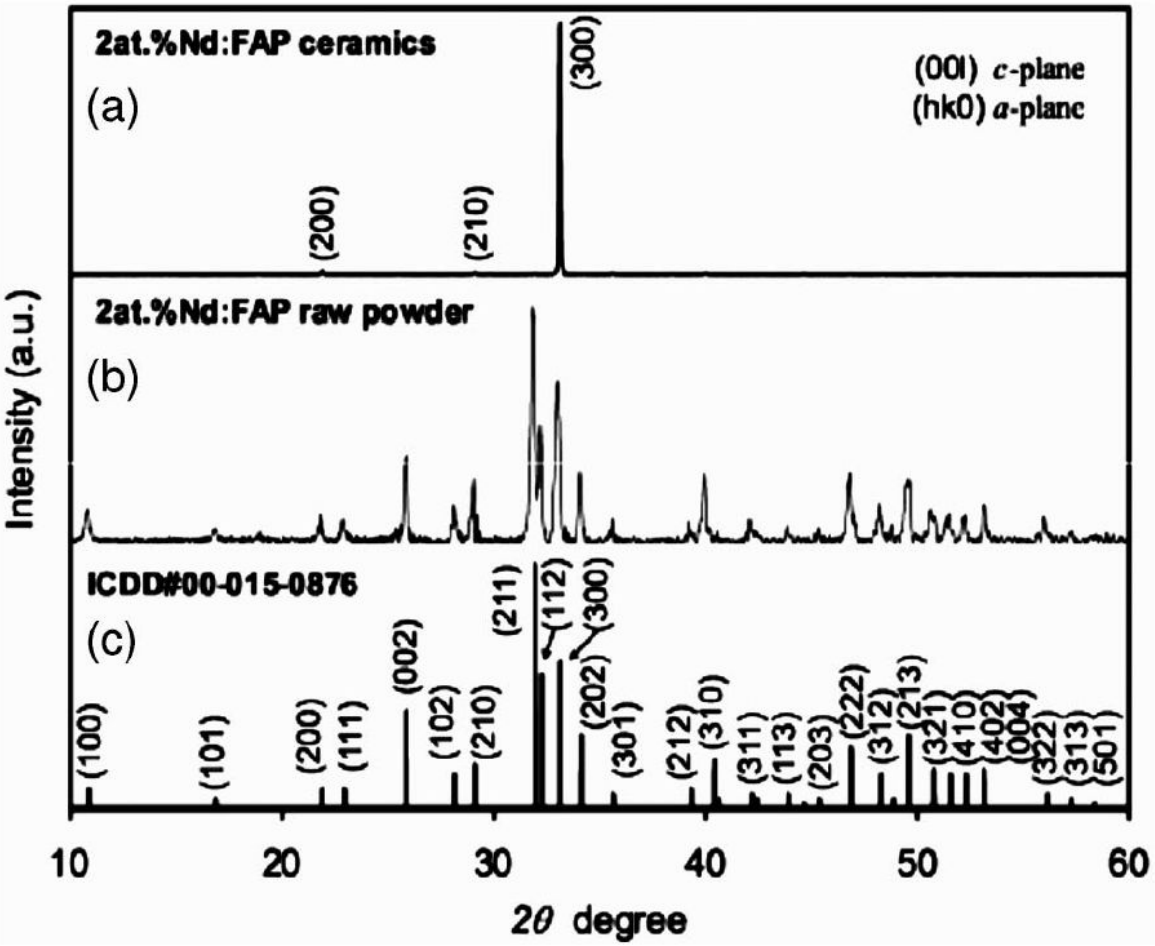

Conclusion

We found the notation of distribution function for crystal orientation under slip-casting.

$$f_{eq}(\theta,\varphi)d\Omega = \frac{N(D)}{4\pi}\frac{2B^2 + B_{\min}(D)^2}{B_{\min}(D)^2}(\cos\theta)^{\frac{2B^2}{B_{\min}(D)^2}}d\Omega$$

We clearly expressed the role of preferential growth for nearly perfect alignment of ceramic grains.

Size distribution of particles is required to be controlled finely.
Viscosity of slurry should be tuned carefully.

We show the possibility for designing magnetic anisotropy and crystal field splitting by controlling local ligand structure around luminous ions.

Thank you for your attention !

Please visit for detailed information: http://taira-web.ims.ac.jp/

This work is partially supported by Genesis Research Institute, Inc.